CRYSTAL GROWTH & DESIGN

Article

pubs.acs.org/crystal

Metal–Organic Framework with Functional Amide Groups for Highly Selective Gas Separation

Shunshun Xiong,[†,‡] Yabing He,[‡,#] Rajamani Krishna,[§] Banglin Chen,*[,‡] and Zhiyong Wang*[,†]

[†]Hefei National Laboratory for Physical Sciences at the Microscale, CAS Key Laboratory of Soft Matter Chemistry and Department of Chemistry, University of Science and Technology of China, Hefei, Anhui, 230026, P. R. China

[‡]Department of Chemistry, University of Texas, One UTSA Circle, San Antonio, Texas 78249-069, United States

[#]College of Chemistry and Life Sciences, Zhejiang Normal University, Jinhua 321004, China

[§]Van't Hoff Institute of Molecular Science, University of Amsterdam, Science Park 904, 1098 XH Amsterdam, The Netherlands

Supporting Information

ABSTRACT: A new three-dimensional microporous metal–organic framework [Cu(*N*-(pyridin-4-yl)isonicotinamide)$_2$(SiF$_6$)](EtOH)$_2$(H$_2$O)$_{12}$ (**UTSA-48**, UTSA = University of Texas at San Antonio) with functional –CONH– groups on the pore surfaces was synthesized and structurally characterized. The small pores and the functional –CONH– groups on the pore surfaces within the activated **UTSA-48a** have enabled their strong interactions with C_2H_2 and CO_2 of adsorption enthalpy of 34.4 and 30.0 kJ mol^{-1}, respectively. Accordingly, activated **UTSA-48** exhibits highly selective gas sorption of C_2H_2 and CO_2 over CH_4 with the Henry Law's selectivities of 53.4 and 13.2 respectively, at 296 K, thereby, highlighting the promise for its application in industrially important gas separation.

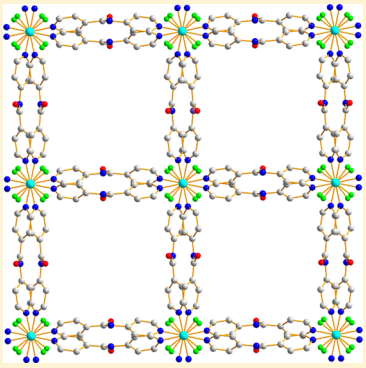

INTRODUCTION

Metal–organic frameworks (MOFs), assembled by organic linkers and inorganic nodes (metal ions or metal-containing clusters), have been emerged as very promising materials for gas storage,[1] gas separation,[2] heterogeneous catalysis,[3] and photoluminescence[4] over the past decades. The diverse selections of organic ligands and inorganic nodes in constructing porous MOFs have allowed us to synthesize an enormeous amounts of porous MOFs in which the pore structures and surface functionality can be systematically tuned for their applications. One of the very promising applications of porous MOFs for gas separation is the selective adsorption of carbon dioxide (CO_2) from other gas components because of their close relevant to environmental and grand energy issues.[5,6] The potential of porous MOFs for the capture and removal of CO_2 via cost-effective and efficient pressure swing adsorption (PSA) and/or thermal swing adsorption (TSA) has initiated the extensive research endeavors to target some highly selective MOF adsorbents for these very important applications.[7] To realize highly selective gas separation, we need to intentionally control the pore/cavity sizes to maximize their size-exclusive effects (small gas molecules can go through the porous channels while big ones are blocked) or to immobilize functional groups (–NH$_2$, –NO$_2$, –OH, –SO$_3$H, open metal sites, etc.) into their pore surfaces for their stronger interactions with CO_2.[7−9]

Pioneered by Zaworotko back in 1995,[10a] a series of isoreticular MOFs of the general formula [M(bpy)$_2$(XF$_6$)] (M = Zn^{2+} and Cu^{2+}; bpy = pyrazine, 4,4′-bipyridine, 1,2-bis(4-pyridyl)-ethene, 4,4′-dipyridylacetylene; X = Si, Ti, Sn) have been demonstrated as excellent CO_2 capture and separation materials.[10] Remarkably, some of these MOF materials can even survive in the humid environments to exhibit highly selective separation without significant sacrifice of the separation capacity.[10d] Given the fact that the functional "–CONH–" groups might enhance their interaction with CO_2 molecules,[11] we incorporated the ligand *N*-(pyridin-4-yl)-isonicotinamide into an isoreticular new MOF and examined its gas separation. Herein, we report a 3D porous MOF [Cu(*N*-(pyridin-4-yl)isonicotinamide)$_2$(SiF$_6$)](EtOH)$_2$(H$_2$O)$_{12}$ (**UTSA-48**) for highly selective C_2H_2/CH_4 and CO_2/CH_4 separation at room temperature.

Scheme 1. Schematic Drawing of the Ligand *N*-(Pyidin-4-yl)isoniconamide

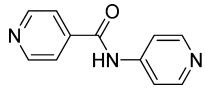

Received: March 25, 2013
Revised: April 19, 2013
Published: April 23, 2013

EXPERIMENTAL SECTION

Materials and Measurements. All reagents and solvents were used as received from commercial suppliers without further purification. Thermogravimetric analyses (TGA) were performed on a Shimadzu TGA-50 analyzer under a nitrogen atmosphere with a heating rate of 3 K min^{-1} from 30 to 800 °C. Powder X-ray diffraction (PXRD) patterns were recorded by a RigakuUltima IV diffractometer operated at 40 kV and 44 mA with a scan rate of 1.0 deg min^{-1}. *N*-(Pyridin-4-yl)isonicotinamide was synthesized according to the literature procedure.[12]

Gas Sorption Measurements. A Micromeritics ASAP 2020 surface area analyzer was used to measure gas adsorption isotherms. To have a guest-free framework, the fresh sample was guest-exchange with dry methanol 3 times per day for 3 days, filtered and vacuumed at 23 °C until the outgas rate was 5 μm Hg min^{-1} prior to measurements. A sample of 111.0 mg was used for the sorption measurements and was maintained at 77 K with liquid nitrogen and at 273 K with an ice–water bath. As the center-controlled air conditioner was set up at 23 °C, a water bath was used for adsorption isotherms at 296 K.

Virial Graph Analysis. Isotherm data were analyzed using the virial equation[13]

$$\ln(n/P) = A_0 + A_1 + A_2 n^2 + \ldots$$

in which P is pressure, n is amount adsorbed, and A_0, A_1, etc., are virial coefficients. A_0 is related to adsorbate–adsorbent interactions. The Henry's law constant (K_H) is equal to $\exp(A_0)$, and selectivity can be obtained from the constant K_H.

Zero Surface Coverage. The isosteric enthalpies of adsorption at zero coverage ($Q_{st,n=0}$) are a fundamental measure of adsorbate–adsorbent interactions, and these values are obtained from the A_0 values obtained by extrapolation of the virial graph to zero surface coverage.

Synthesis of UTSA-48. Crystals of **UTSA-48** were formed by layering a solution of 20 mg of *N*-(pyridin-4-yl)isonicotinamide in 1 mL of EtOH onto a solution containing 17.3 mg of $Cu(BF_4)_2$ and 8.91 mg of $(NH_4)_2SiF_6$ in 2 mL of H_2O. Purple, rectangular crystals grow after one week. **UTSA-48** was formulated as $[Cu(N\text{-(pyridin-4-yl)isonicotinamide})_2(SiF_6)](EtOH)_2(H_2O)_{12}$ on the basis of the TGA and element analysis. Calcd: C 36.66%, H 6.37%, N 3.27%; Found C 36.84%, H 6.19%, N 3.56%.

Single-Crystal X-ray Structure Determination. Single crystal X-ray diffraction was performed with an Oxford Diffraction Gemini S Ultra CCD diffractometer equipped with graphite-monochromated Cu–Kα (λ =1.54184 Å) using "multiscan" technique. X-Stream low temperature device was used to keep the crystals at a constant 180(2) K during data collection. The structure was solved by WinGX and refined by a matrix least-squares method using SHELXL-97 programs.[14] The non-hydrogen atoms were refined anisotropically. Disordered, independent solvent molecules inside the frameworks were eliminated in the refinement by PLATON/SQUEEZE.[15]

RESULTS AND DISCUSSION

UTSA-48 crystallizes in the tetragonal space group *P4/ncc*. The copper center is octahedrally coordinated by the four nitrogen atoms of the *N*-(pyridin-4-yl)isonicotinamide ligands and further by the two SiF_6^{2-} ions. The *N*-(pyridin-4-yl)-isonicotinamide ligands bridge copper ions into grids layers in the equatorial plane and SiF_6^{2-} ions pillar the 2D layers into a **pcu** framework with square channels along the *c* axis. The void volume in **UTSA-48** is 27.7% calculated by PLATON.[15] Compared with $[Cu(bpy\text{-}n)_2(SiF_6)]$ (bpy-1 = 4,4′-bipyridine; bpy-2 = 1,2-bis(4-pyridyl)-ethene), bpe),[10b] *N*-(pyridin-4-yl)isonicotinamide in **UTSA-48** is nearly the same length as bpe and a little longer than 4,4′-bipyridine. The effective windows size of the channels in **UTSA-48** considering the van der Waals radii of the framework atoms is only 8 Å. This value is the similar as $[Cu(bpy\text{-}1)_2(SiF_6)]$ and smaller than $[Cu(bpy\text{-}2)_2(SiF_6)]$ (10.6 Å). This could be attributed to the flexibility and distortion of the *N*-(pyridin-4-yl)isonicotinamide ligand in the framework.

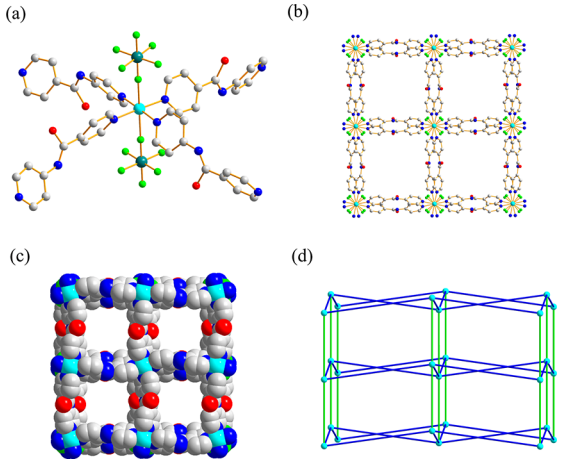

Figure 1. (a) Coordination environment of Cu center (carbon, gray; oxygen, red; nitrogen, blue; copper, cyan; silicon, olive; fluorine, green). (b) Tetragonal crystal structure of **UTSA-48** indicating the square channels along the crystallographic *c* axis. (c) A space-filling model showing nanosized channels viewed along the *c*-axis; (d) Schematic view of the **pcu** topology framework of **UTSA-48**. For clarity, the linkers are displayed in two colors: the blue straight linkers represent *N*-(pyridin-4-yl)isonicotinamide ligands, and the green straight linkers represent SiF_6^{2-} anions. The cyan nodes represent Cu centers.

Thermogravimetric analysis (TGA) of **UTSA-48** showed that approximately 36.41% weight loss occurred from 21 to 100 °C, which is attributed to the release of solvent molecules. Methanol-exchanged **UTSA-48** was activated at room temperature under high vacuum to obtain the activated sample **UTSA-48a**. The N_2 sorption isotherm of **UTSA-48a** at 77 K indicates a typical type I but two step hysteresis sorption behavior. Many reported MOFs especially flexible/dynamic MOFs have exhibited this unique sorption behavior because of the phase transitions and the metastable intermediate phase.[16] Such hysteresis N_2 sorption is apparently attributed to the flexible nature of the ligand *N*-(pyridin-4-yl)isonicotinamide. Such flexibility also significantly reduce the porosity of the framework, as clearly shown in the much lower N_2 uptake of 135.2 $cm^3\ g^{-1}$ (STP) at 77 K and thus much lower surface area of 285 $m^2\ g^{-1}$ in **UTSA-48a** compared with 1346 $m^2\ g^{-1}$ in $[Cu(bpy\text{-}1)_2(SiF_6)]$ and 1468 $m^2\ g^{-1}$ in $[Cu(bpy\text{-}2)_2(SiF_6)]$.[10] The hydrogen adsorption isotherm indicates an uptake of 65.8 $cm^3\ g^{-1}$ (0.59 wt %) at 77 K and 1 atm (Figure 2).

The establishment of the permanent porosity enabled us to examine their gas sorptions of C_2H_2, CO_2, and CH_4. As shown in Figure 3, **UTSA-48a** takes up moderate amounts of acetylene (40 $cm^3\ g^{-1}$) and carbon dioxide (28 $cm^3\ g^{-1}$), which are much higher than that of methane (4.4 $cm^3\ g^{-1}$) at 296 K and 1 atm. On the basis of their sorption isotherms at 273 and 296 K, we examined the potential of this new MOF for C_2H_2/CH_4, and CO_2/CH_4 separation. The corresponding virial parameters are given in Table 1. The isosteric enthalpies of adsorption ($Q_{st,n=0}$) at zero surface coverage for C_2H_2, CO_2, and CH_4 were 34.4, 30.0, and 16.9 kJ mol^{-1}, respectively. The acetylene enthalpy of **UTSA-48a** is higher than **HKUST-1** (30.4 kJ mol^{-1}) with large pores and open metal sites.[17] The fact that the $Q_{st,n=0}$ of **UTSA-48a** for CO_2 is higher than the values of $[Cu(bpy\text{-}1)_2(SiF_6)]$

dx.doi.org/10.1021/cg4004438 | *Cryst. Growth Des.* 2013, 13, 2670–2674

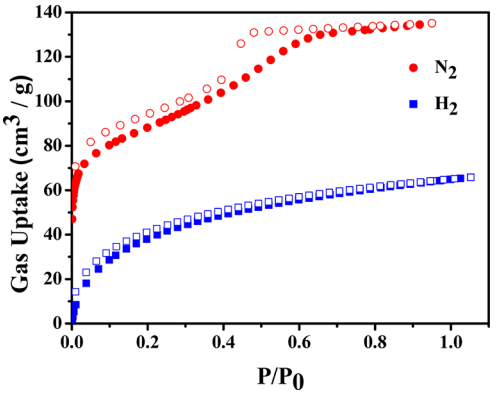

Figure 2. Adsorption isotherms of N_2 (red circle) and H_2 (blue square) gases on **UTSA-48a** at 77 K.

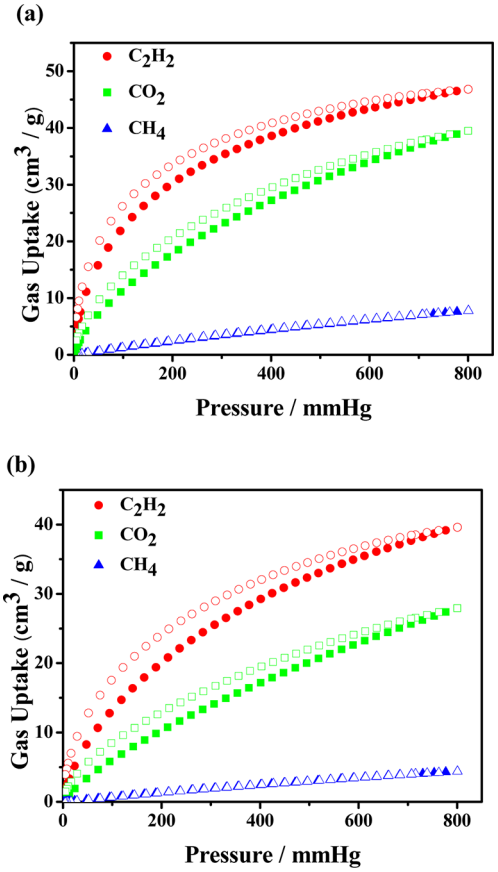

Figure 3. Adsorption (solid) and desorption (open) isotherms of acetylene (red circles), carbon dioxide (green squares), and methane (blue triangles) on **UTSA-48a** at 273 (a) and 296 K (b).

(27 kJ mol^{-1}) and [Cu(bpy-2)$_2$(SiF$_6$)] (22 kJ mol^{-1}) indicates that immobilized functional amide groups on the pore surfaces of **UTSA-48a** can enhance their interactions with CO_2 gas molecules which has been also observed in another MOF by Bai's groups.[11] The Henry's Law selectivity for C_2H_2/CH_4, calculated based on the equation $S_{i/CH4} = K_{H(i)}/K_{H(CH_4)}$, are 97.2 and 53.4 at 273 and 296 K, respectively, which are much higher than most MOFs.[2h] **UTSA-48a** exhibits higher CO_2/CH_4 separation with a Henry's Law selectivity of 20.7 and 13.2 at 273 and 296 K, respectively, than [Cu(bpy-1)$_2$(SiF$_6$)] and [Cu(bpy-2)$_2$(SiF$_6$)].[10] The separation capacity of **UTSA-48a** for the selective CO_2/CH_4 separation has been further examined by the ideal adsorbed solution theory (IAST). The accuracy of IAST for prediction of gas mixture adsorption in a large number of zeolites and MOFs has been well established.[18] The CO_2/CH_4 selectivity of **UTSA-48a** decrease with increasing bulk pressure (Figure 4). The functional amide

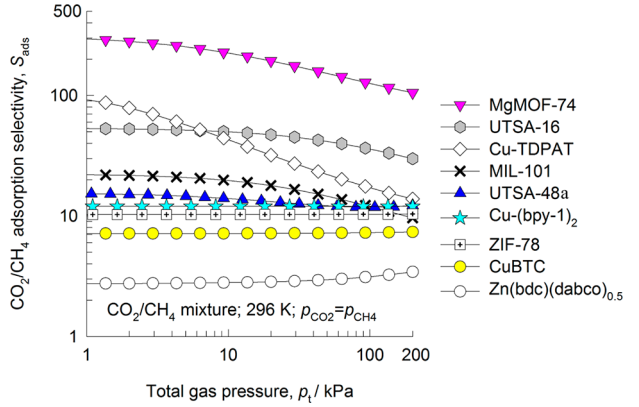

Figure 4. CO_2/CH_4 adsorption selectivity for the variety of MOFs considered in this work. Cu-(BPY-1) represent [Cu(bpy-1)$_2$(SiF$_6$)]. In these calculations, the partial pressures of CO_2 and CH_4 are taken to be equal to each other, that is, $p_1 = p_2$.

groups play more important roles for their stronger interactions with CO_2 under low pressure than high pressure. The selectivity is comparable to the value calculated by Henry's law. We further compared the CO_2/CH_4 adsorption selectivties examined by IAST for the different MOFs at 296 K. As shown in Figure 4, **UTSA-48a** has a higher selectivity than Cu-(bpy-1)$_2$ ([Cu(bpy-1)$_2$(SiF$_6$)]), ZIF-78, CuBTC, and Zn(bdc)-(dabco)$_{0.5}$, and a lower one than MgMOF-74, UTSA-16, Cu-TDPAT, and MIL-101. The specific orbital interactions of CO_2 molecules with the open Mg atoms makes Mg-MOF-74 the highest selectivity among the reported MOFs.[8d] The second highest selectivity of UTSA-16 for CO_2/CH_4 is attributed to the optimal pore cages and the strong binding sites to the CO_2

Table 1. Virial Graph Analyses Data for UTSA-48a and Its CO_2/CH_4 and C_2H_2/CH_4 Separation Selectivities

adsorbate	T (K)	K_H (mol g^{-1} Pa^{-1})	A_0 (ln(mol g^{-1} Pa^{-1})	A_1 (g mol^{-1})	R^2	$S_{i/CH4}$[a]	Q_{st} (kJ mol^{-1})
C_2H_2	273	4.213×10^{-7}	−14.679	−2124.816	0.9882	97.2	34.4
	296	1.298×10^{-7}	−15.858	−2698.676	0.9995	53.4	
CO_2	273	8.969×10^{-8}	−16.227	−2116.797	0.9968	20.7	30.0
	296	3.216×10^{-8}	−17.253	−2190.012	0.9896	13.2	
CH_4	273	4.333×10^{-9}	−19.257	−874.097	0.9980		16.9
	296	2.430×10^{-9}	−19.835	−1603.285	0.9918		

[a]The Henry's law selectivity for gas component i over CH4 at the speculated temperature is calculated based on the equation Si/CH4= KH(i)/KH(CH4).

dx.doi.org/10.1021/cg4004438 | Cryst. Growth Des. 2013, 13, 2670−2674

molecules.[7e] **UTSA-48a** exhibits higher CO_2/CH_4 selectivity than $[Cu(bpy\text{-}1)_2(SiF_6)]$ by immobilizing −CONH− sites to induce their strong interactions with CO_2. This also indicates that −CONH− groups have the same positive effect on adsorption of CO_2 like the widely reported $-NH_2$ groups by facilitating dipole−quadrupole interactions between −CONH− groups and CO_2 or NH···OCO hydrogen bonds.[8,9,11] However, these two analogous function groups have some different structural and chemical characteristics. The −CONH− group usually does not coordinate with metal ions and keeps open status in process of constructing MOFs, although it may increase the structural flexibility of MOFs because of its customary position in the main carbon skeleton of the organic ligands. While, the $-NH_2$ group may coordinate with metal ions and loses its function to interact with CO_2 when the organic ligands with $-NH_2$ groups are employed in synthesizing MOFs. On the other hand, the $-NH_2$ group is not located on the main carbon skeleton of the organic ligands and has no apparent influence on the rigidity or flexibility of the MOFs' stuctures. Therefore, it is important to choose appropriate functional groups to design and synthesize MOFs according to their chemical and structural nature. The breakthrough calculation indicates that **UTSA-48a** has a τ_{break} of 29 (Supporting Information Figure S5). This value is lower than most MOFs considered in this work due to its lower porosity.

CONCLUSION

In summary, we have successfully synthesized a new 3D microporous MOF **UTSA-48** with immobilized −CONH− functional groups on the pore surfaces. Such functional −CONH− groups induce their strong interactions with C_2H_2 and CO_2, which lead to high Henry's law selectivities of **UTSA-48a** for C_2H_2/CH_4 (53.4) and CO_2/CH_4 (13.2) at 296 K. This work once again confirms that the functional organic groups can play important roles to adjust their interactions with gas molecules. By tuning the pore structures and immobilizing functional sites onto the pore surfaces, some more promising MOF materials will be realized for some important gas separation such as CO_2/CH_4 and C_2H_2/CH_4 in the near future.

ASSOCIATED CONTENT

Supporting Information

PXRD patterns, TGA curves, and crystallographic data (CCDC 927436) for **UTSA-48**. This material is available free of charge via the Internet at http://pubs.acs.org.

AUTHOR INFORMATION

Corresponding Author

*E-mail: Banglin.Chen@utsa.edu (B.C.); zwang3@ustc.edu.cn (Z.W.). Fax 1-210-458-7428 (B.W.).

Notes

The authors declare no competing financial interest.

ACKNOWLEDGMENTS

We are thankful for China Scholarship Council. This work was supported by the National Nature Science Foundation of China (21272222, 21172205, 20972144, 20932002, 91213303, and J1030412), Grant AX-1730 from the Welch Foundation (BC), and from the Ministry of Science and Technology of China (2010CB912103).

REFERENCES

(1) (a) Banerjee, R.; Phan, A.; Wang, B.; Knobler, C.; Furukawa, H.; O'Keeffe, M.; Yaghi, O. M. *Science* **2008**, *319*, 939. (b) Kitagawa, S.; Kitaura, R.; Noro, S.-I. *Angew. Chem., Int. Ed.* **2004**, *43*, 2334. (c) Matsuda, R.; Kitaura; Kitagawa, S.; Kubota, Y.; Belosludov, R. V.; Kobayashi, T. C.; Sakamoto, H.; Chiba, T.; Takata, M.; Kawazoe, Y.; Mita, Y. *Nature* **2005**, *436*, 238. (d) Millward, A. R.; Yaghi, O. M. *J. Am. Chem. Soc.* **2005**, *127*, 17998. (e) Murray, L. J.; Dinca, M.; Long, J. R. *Chem. Soc. Rev.* **2009**, *38*, 1294. (f) Férey, G. *Chem. Soc. Rev.* **2008**, *37*, 191. (g) Ma, S.; Sun, D.; Simmons, J. M.; Collier, C. D.; Yuan, D.; Zhou, H.-C. *J. Am. Chem. Soc.* **2008**, *130*, 1012. (h) Wu, H.; Zhou, W.; Yildirim, T. *J. Am. Chem. Soc.* **2009**, *131*, 4995. (i) Chen, B.; Ockwig, N. W.; Millward, A. R.; Contreras, D. S.; Yaghi, O. M. *Angew. Chem., Int. Ed.* **2005**, *44*, 4745. (j) Guo, Z.; Wu, H.; Srinivas, G.; Zhou, Y.; Xiang, S.; Chen, Z.; Yang, Y.; Zhou, W.; O'Keeffe, M.; Chen, B. *Angew. Chem., Int. Ed.* **2011**, *50*, 3178. (k) Xiang, S.; Zhou, W.; Zhang, Z.; Green, M. A.; Liu, Y.; Chen, B. *Angew. Chem., Int. Ed.* **2010**, *49*, 4615.

(2) (a) Li, J.-R.; Sculley, J.; Zhou, H.-C. *Chem. Rev.* **2012**, *112*, 869. (b) Sumida, K.; Rogow, D. L.; Mason, J. A.; McDonald, T. M.; Bloch, E. D.; Herm, Z. R.; Bae, T.-H.; Long, J. R. *Chem. Rev.* **2012**, *112*, 724. (c) Zhang, Z.; Zhao, Y.; Gong, Q.; Li, Z.; Li, J. *Chem. Commun.* **2013**, *49*, 653. (d) Ma, S.; Zhou, H.-C. *Chem. Commun.* **2010**, *46*, 44. (e) Bae, Y.-S.; Snurr, R. Q. *Angew. Chem., Int. Ed.* **2011**, *50*, 11586. (f) Wu, H.; Gong, Q.; Olson, D. H.; Li, J. *Chem. Rev.* **2012**, *112*, 836. (g) Jiang, H.-L.; Xu, Q. *Chem. Commun.* **2011**, *47*, 3351. (h) Chen, B.; Xiang, S.; Qian, G. *Acc. Chem. Res.* **2010**, *43*, 1115. (i) Zhang, Z.; Xiang, S.; Chen, B. *CrystEngComm* **2011**, *13*, 5983. (j) He, Y.; Zhou, W.; Krishna, R.; Chen, B. *Chem. Commun.* **2012**, *48*, 11813. (k) He, Y.; Zhang, Z.; Xiang, S.; Wu, H.; Fronczek, F. R.; Zhou, W.; Krishna, R.; O'Keeffe, M.; Chen, B. *Chem.—Eur. J.* **2012**, *18*, 1901.

(3) (a) Seo, J. S.; Whang, D.; Lee, H.; Jun, S. I.; Oh, J.; Jeon, Y. J.; Kim, K. *Nature* **2000**, *404*, 982. (b) Wu, C.-D.; Hu, A.; Zhang, L.; Lin, W. *J. Am. Chem. Soc.* **2005**, *127*, 8940. (c) Horike, S.; Dincă, M.; Tamaki, K.; Long, J. R. *J. Am. Chem. Soc.* **2008**, *130*, 5854. (d) Banerjee, M.; Das, S.; Yoon, M.; Choi, H. J.; Hyun, M. H.; Park, S. M.; Seo, G.; Kim, K. *J. Am. Chem. Soc.* **2009**, *131*, 7524. (e) Ma, L.; Abney, C.; Lin, W. *Chem. Soc. Rev.* **2009**, *38*, 1248. (f) Corma, A.; García, H.; Llabrés i Xamena, F. X. *Chem. Rev.* **2010**, *110*, 4606. (g) Lee, J.; Farha, O. K.; Roberts, J.; Scheidt, K. A.; Nguyen, S. T.; Hupp, J. T. *Chem. Soc. Rev.* **2009**, *38*, 1450. (h) Aijaz, A.; Karkamkar, A.; Choi, Y. J.; Tsumori, N.; Rönnebro, E.; Autrey, T.; Shioyama, H.; Xu, Q. *J. Am. Chem. Soc.* **2012**, *134*, 13926.

(4) (a) Allendorf, M. D.; Bauer, C. A.; Bhakta, R. K.; Houk, R. J. T. *Chem. Soc. Rev.* **2009**, *38*, 1330. (b) Lee, E. Y.; Jang, S. Y.; Suh, M. P. *J. Am. Chem. Soc.* **2005**, *127*, 6374. (c) Lin, J.-G; Xu, Y. Y.; Qiu, L.; Zang, S.-Q.; Lu, C.-S.; Duan, C.-Y.; Li, Y.-Z.; Gao, S.; Meng, Q.-J. *Chem. Commun.* **2008**, 2659. (d) Park, Y. K.; Choi, S. B.; Kim, H.; Kim, K.; Won, B. H.; Choi, K.; Choi, J. S.; Ahn, W. S.; Won, N.; Kim, S.; Jung, D. H.; Choi, S. H.; Kim, G. H.; Cha, S. S.; Jhon, Y. H.; Yang, J. K.; Kim, J. *Angew. Chem., Int. Ed.* **2007**, *46*, 8230. (e) Bai, Y.; He, G. J.; Zhao, Y. G.; Duan, C. Y.; Dang, D. B.; Meng, Q. J. *Chem. Commun.* **2006**, 1530. (f) Chen, B. L.; Wang, L. B.; Zapata, F.; Qian, G. D.; Lobkovsky, E. B. *J. Am. Chem. Soc.* **2008**, *130*, 6718. (g) Huang, Y.-Q.; Ding, B.; Song, H.-B.; Zhao, B.; Ren, P.; Cheng, P.; Wang, H.-G.; Liao, D.-Z.; Yan, S.-P. *Chem. Commun.* **2006**, 4906. (h) Stylianou, K. C.; Heck, R.; Chong, S. Y.; Bacsa, J.; Jones, J. T.; Khimyak, Y. Z.; Bradshaw, D.; Rosseinsky, M. J. *J. Am. Chem. Soc.* **2010**, *132*, 4119. (i) Liu, Q.-K.; Ma, J.-P.; Dong, Y.-B. *Chem.—Eur. J.* **2009**, *15*, 10364. (j) Lan, A.; Li, K.; Wu, H.; Olson, D. H.; Emge, T. J.; Ki, W.; Hong, M.; Li, J. *Angew, Chem., Int. Ed.* **2009**, *48*, 2334. (l) Cui, Y. J.; Xu, H.; Yue, Y. F.; Guo, Z. Y.; Yu, J. C.; Chen, Z. X.; Gao, J. K.; Yang, Y.; Qian, G. D.; Chen, B. L. *J. Am. Chem. Soc.* **2012**, *134*, 3979.

(5) (a) Keller, J.; Staudt, R. *Gas Adsorption Equilibria: Experimental Methods and Adsorptive Isotherms*; Springer: New York, 2004. (b) Keskin, S.; van Heest, T. M.; Sholl, D. S. *ChemSusChem* **2010**, *3*, 879. (c) Kerry, F. G. *Industrial Gas Handbook: Gas Separation and Purification*; CRC Press: Boca Raton, 2007.

(6) (a) Rochelle, G. T. *Science* **2009**, *325*, 1652. (b) Haszeldine, R. S. *Science* **2009**, *325*, 1647.

(7) (a) Bastin, L.; Barcia, P. S.; Hurtado, E. J. J.; Silva, A. C.; Rodrigues, A. E.; Chen, B. *J. Phys. Chem. C* **2008**, *112*, 1575. (b) Ma, S.; Wang, X. S.; Collier, C. D.; Manis, E. S.; Zhou, H. C. *Inorg. Chem.* **2007**, *46*, 8499. (c) Cheon, Y. E.; Suh, M. P. *Chem. Commun.* **2009**, 2296. (d) Das, M. C.; Xu, H.; Xiang, S.; Zhang, Z.; Arman, H. D.; Qian, G.; Chen, B. *Chem.—Eur. J.* **2011**, *17*, 7817. (e) Xiang, S.; He, Y.; Zhang, Z.; Wu, H.; Zhou, W.; Krishna, R.; Chen, B. *Nat. Commun.* **2012**, *3*, 954. (f) Ling, Y.; Deng, M.; Chen, Z.; Xia, B.; Liu, X.; Yang, Y.; Zhou, Y.; Weng, L. *Chem. Commun.* **2013**, *49*, 78. (g) Zhang, Z.; Xiang, S.; Hong, K.; Madhab, C. D.; Arman, H. D.; Garcia, M.; Mondal, J. U.; Thomas, K. M.; Chen, B. *Inorg. Chem.* **2012**, *51*, 4947. (h) Chen, B.; Ma, S.; Zapata, F.; Fronczek, F. R.; Lobkovsky, E. B.; Zhou, H.-C. *Inorg. Chem.* **2007**, *46*, 1233.

(8) (a) Vimont, A.; Goupil, J.-M.; Lavalley, J.-C.; Daturi, M.; Surblé, S.; Serre, C.; Millange, F.; Férey, G.; Audebrand, N. *J. Am. Chem. Soc.* **2006**, *128*, 3218. (b) Dietzel, P. D. C.; Besikiotis, V.; Blom, R. *J. Mater. Chem.* **2009**, *19*, 7362. (c) Caskey, S. R.; Wong-Foy, A. G.; Matzger, A. J. *J. Am. Chem. Soc.* **2008**, *130*, 10870. (d) Llewellyn, P. L.; Bourrelly, S.; Serre, C.; Vimont, A.; Daturi, M.; Hamon, L.; Weireld, G. D.; Chang, J.-S.; Hong, D.-Y.; Hwang, Y. K.; Férey, G. *Langmuir.* **2008**, *24*, 7245. (e) Liu, J.; Wang, Y.; Benin, A. I.; Jakubczak, P.; Willis, R. R.; LeVan, M. D. *Langmuir.* **2010**, *26*, 4301. (f) Aprea, P.; Caputo, D.; Gargiulo, N.; Iucolano, F.; Pepe, F. J. *Chem. Eng. Data.* **2010**, *55*, 3655. (g) Panda, T.; Pachfule, P.; Chen, Y.; Jiang, J.; Banerjee, R. *Chem. Commun.* **2011**, *47*, 2011. (h) Pachfule, P.; Chen, Y.; Jiang, J.; Banerjee, R. *J. Mater. Chem.* **2011**, *21*, 17737.

(9) (a) Furukawa, H.; Kim, J.; Ockwig, N. W.; O'Keefe, M.; Yaghi, O. M. *J. Am. Chem. Soc.* **2008**, *130*, 11650. (b) Lin, Q.; Wu, T.; Zheng, S.-T.; Bu, X.; Feng, P. *J. Am. Chem. Soc.* **2012**, *134*, 784. (c) Kim, T. K.; Suh, M. P. *Chem. Commun.* **2011**, *47*, 4258. (d) Banerjee, R.; Furukawa, H.; Britt, D.; Knobler, C.; O'Keeffe, M.; Yaghi, O. M. *J. Am. Chem. Soc.* **2009**, *131*, 3875. (e) Neofotistou, E.; Malliakas, C. D.; Trikalitis, P. N. *Chem.—Eur. J.* **2009**, *15*, 4523. (f) Tian, Y.-Q.; Yao, S.-Y.; Gu, D.; Cui, K.-H.; Guo, D.-W.; Zhang, G.; Chen, Z.-X.; Zhao, D.-Y. *Chem.—Eur. J.* **2010**, *16*, 1137. (g) Liu, X.-M.; Lin, R.-B.; Zhang, J.-P.; Chen, X.-M. *Inorg. Chem.* **2012**, *51*, 5686. (h) Mallick, A.; Kundu, T.; Banerjee, R. *Chem. Commun.* **2012**, *48*, 8829. (i) Chen, Z.; Xiang, S.; Arman, H.-D.; Li, P.; Zhao, D.; Chen, B. *Eur. J. Inorg. Chem.* **2011**, *14*, 2227. (j) An, J.; Geib, S. J.; Rosi, N. L. *J. Am. Chem. Soc.* **2010**, *132*, 38. (k) Wang, F.; Tan, Y.-X.; Yang, H.; Kang, Y.; Zhang, J. *Chem. Commun.* **2012**, *48*, 4842. (l)

(10) (a) Subramanian, S.; Zaworotko, M. J. *Angew. Chem., Int. Ed.* **1995**, *34*, 2127. (b) Burd, S. D.; Ma, S.; Perman, J. A.; Sikora, B. J.; Snurr, R. Q.; Thallapally, P. K.; Tian, J.; Wojtas, L.; Zaworotko, M. J. *J. Am. Chem. Soc.* **2012**, *134*, 3663. (c) Nugent, P.; Rhodus, V.; Pham, T.; Tudor, B.; Forrest, K.; Wojtas, L.; Space, B.; Zaworotko, M. *Chem.Commun.* **2013**, *49*, 1606. (d) Nugent, P.; Belmabkhout, Y.; Burd, S. D.; Cairns, A. J.; Luebke, R.; Forrest, K.; Pham, T.; Ma, S.; Space, B.; Wojtas, L.; Mohamed, E.; Zaworotko, M. J. *Nature* **2013**, *495*, 80−84.

(11) (a) Lu, Z.; Xiang, H.; Sun, R.; Bai, J.; Zheng, B.; Li, Y. *Cryst. Growth Des.* **2012**, *12*, 1081. (b) Zheng, B.; Yang, Z.; Bai, J.; Li, Y.; Li, S. *Chem Commun.* **2012**, *48*, 7025. (c) Zheng, B.; Bai, J.; Duan, J.; Wojtas, L.; Zaworotko, M. J. *J. Am. Chem. Soc.* **2011**, *133*, 748.

(12) Qin, Z.; Jennings, M. C.; Puddephat, R. J. *Chem. Commum.* **2001**, 2676.

(13) (a) Rowsell, J. L. C.; Yaghi, O. M. *J. Am. Chem. Soc.* **2006**, *128*, 1304. (b) Jagiello, J.; Bandosz, T. J.; Putyera, K.; Schwarz, J. A. *J. Chem. Eng. Data* **1995**, *40*, 1288. (c) Chen, B.; Zhao, X.; Putkham, A.; Hong, K.; Lobkovsky, E. B.; Hurtado, E. J.; Fletcher, A. J.; Thomas, K. M. *J. Am. Chem. Soc.* **2008**, *130*, 6411. (d) Zhao, V.-R.; Fletcher, A. J.; Thomas, K. M. *J. Phys. Chem. B.* **2006**, *110*, 9947.

(14) Sheldrick, G. M. *SHELXL-97, Program for Crystal Structure Refinement*; Göttingen University: Göttingen, Germany, 1997.

(15) Spek, L. *PLATON*; The University of Utrecht: Utrecht, the Netherlands, 1999.

(16) Uemura, K.; Yamasaki, Y.; Onishi, F.; Kita, H.; Ebihara, M. *Inorg. Chem.* **2010**, *49*, 10133.

(17) Xiang, S.-C.; Zhou, W.; Gallegos, J. M.; Liu, Y.; Chen, B. *J. Am. Chem. Soc.* **2009**, *131*, 12415.

(18) Krishna, R.; Van Baten, J. M. *Phys. Chem. Chem. Phys.* **2011**, *13*, 10593.

Supporting Information for the Manuscript

A Metal-Organic Framework with Functional Amide Groups for Highly Selective Gas Separation

ShunshunXiong, [†,‡] *Yabing He* [‡], *Rajamani Krishna* [§], *Banglin Chen** [‡], *Zhiyong Wang** [†]

[†]*Hefei National Laboratory for Physical Sciences at the Microscale, CAS Key Laboratory of Soft Matter Chemistry and Department of Chemistry, University of Science and Technology of China, Hefei, Anhui, 230026, P. R. China. E-mail: zwang3@ustc.edu.cn*

[‡]*Department of Chemistry, University of Texas at San Antonio, One UTSA Circle, San Antonio, Texas 78249-069, United States. Fax (1)-210-458-7428; E-mail: Banglin.Chen@utsa.edu.*

[§]*Van't Hoff Institute of Molecular Science, University of Amsterdam, Science Park 904, 1098 XH Amsterdam, The Netherlands.*

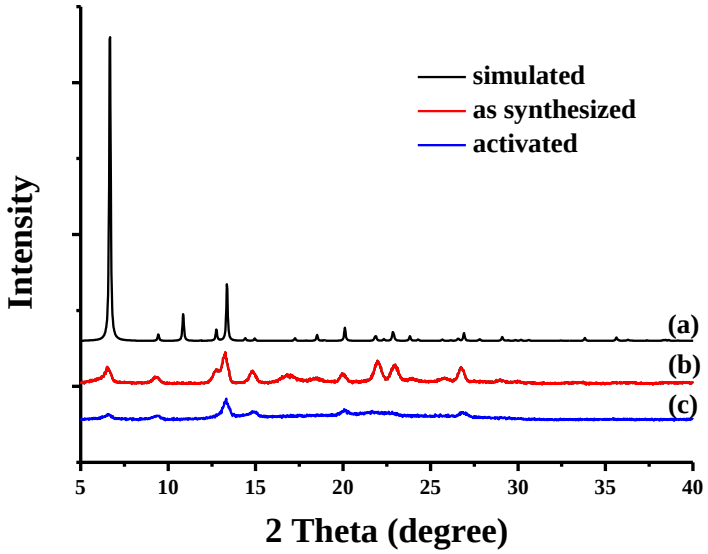

Figure S1. PXRD patterns of as-synthesized **UTSA-48** (b) and activated **UTSA-48a** (c) along with the simulated pattern from its single crystal X-ray structure (a).

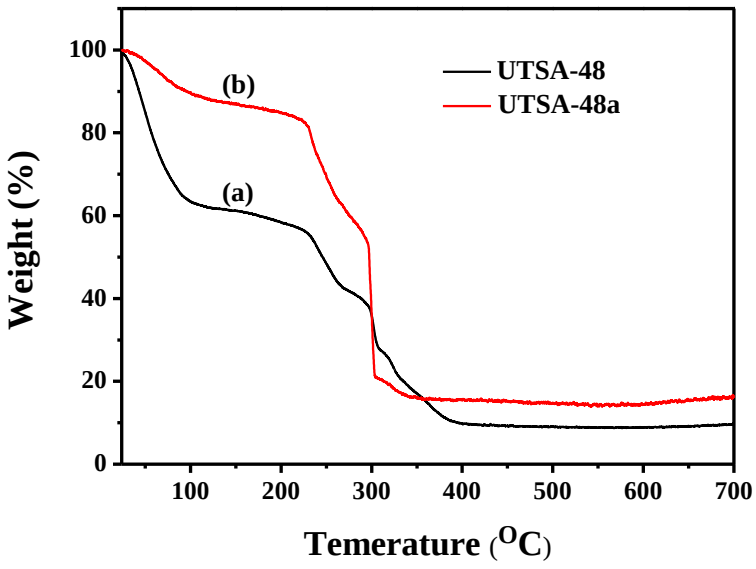

Figure S2. TGA curves of as-synthesized **UTSA-48** (a) and activated **UTSA-48a** (b)

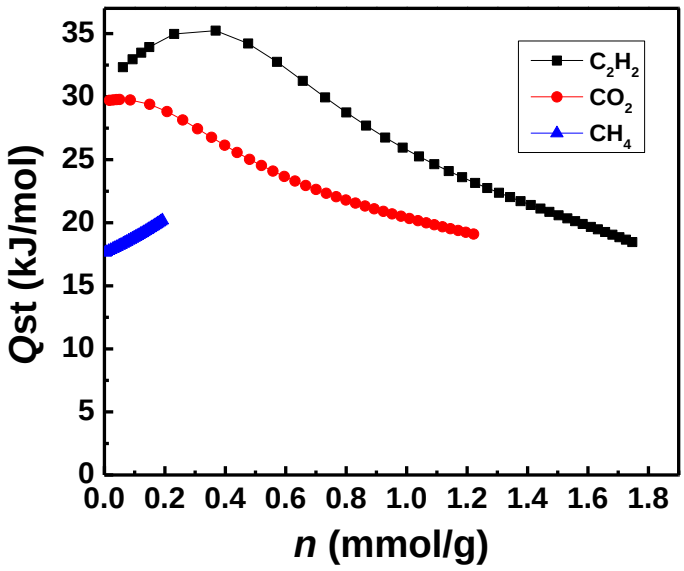

Figure S3. Isoteric heats of C_2H_2, CO_2 and CH_4 adsorption for **UTSA-48a**

Table S1. Crystal data and structure refinement for **UTSA-48**

Empirical Formula	$C_{24}H_{18}Cu_1F_6N_4O_4Si_1$
Formula weight	632.06
Temperature (K)	180
Wavelength (Å)	1.54184
Crystal system, space group	Tetragonal, P4/ncc
Unit cell dimensions	a = 18.2679(3) Å, α = 90°
	b = 18.2679(3) Å, β = 90°
	c = 15.9522(5) Å, γ = 90°
Volume ($Å^3$)	5323.5(2)
Z , Calculated density (gcm^{-3})	4, 0.789

Absorption coefficient (mm^{-1})	1.165
$F(000)$	1276.0
Crystal size (mm)	0.36 × 0.33 × 0.31
θ range for data collection	4.84 to 66.42°
R_{int}	0.046
Total/independent reflns	8660/2300
Completeness	97.7 %
Parameters	107
Refinement method	Full-matrix least-squares on F^2
Goodness-of-fit on F^2 [c]	1.088
R^a, R_w [b]	R1 = 0.0812, wR2 = 0.2189
R indices (all data)	R1 = 0.0943, wR2 = 0.2280

[a] $R = \Sigma||F_o| - |F_c|| / \Sigma|F_o|$. [b] $R_w = [\Sigma[w(F_o^2 - F_c^2)^2] / \Sigma w(F_o^2)^2]^{1/2}$. [c] GOF = $\{\Sigma[w(F_o^2 - F_c^2)^2]/(n - p)\}^{1/2}$.

Ideal Adsorbed Solution Theory:

The ideal adsorbed solution theory (IAST)[1] was used to predict the equimolar binary mixture adsorption of CO_2 and CH_4 from the experiment pure-gas isotherm. The single-component isotherms were fit to a dual-site Langmuir-Freundlich equation:

$$q = q_{m1} \bullet \frac{b_1 \bullet P^{1/n_1}}{1 + b_1 \bullet P^{1/n_1}} + q_{m2} \bullet \frac{b_2 \bullet P^{1/n_2}}{1 + b_2 \bullet P^{1/n_2}} \qquad (1)$$

Here, P is the pressure of the bulk gas at equilibrium with the adsorbed phase (kPa), q is the adsorbed amount per mass of adsorbent (mol/kg), q_{m1} and q_{m2} are the saturation capacities of sites 1 and 2 (mol/kg). b_1 and b_2 are affinity coefficient of sites 1 and 2 (1/kPa), and n_1 and n_2

represent the deviations from an ideal homogeneous surface. Although this is not the only model that can be used to fit the data, IAST requires a precise fit of the experimental data to the model in order to accurately perform the necessary integrations.[2-4]

[1] Myers, A. L.; Prausnitz, J. M. *AIChE J.* **1965**, *11*, 121.

[2] Babarao, R.; Hu, Z. Q.; Jiang J. W.; Chempath, S.; Sandler, S. I. *Langmuir,* **2007**, *23*, 659.

[3] Goetz, V.; Pupier, O.; Guillot, A. *Adsorption*, **2006**, *12*, 55.

[4] Bae, Y. S.; Mulfort K. L.; Frost, H.; Ryan, P.; Punnathanam, S.; Broadbelt, L. J.; Hupp, J. T.; Snurr, R. Q. *Langmuir,* **2008**, *24*, 8592.

Breakthrough Calculation

The breakthrough calculations were performed using the following the methodologies developed in earlier works. Assuming plug flow of CO_2(1)/CH_4(2) gas mixture through a fixed bed maintained under isothermal conditions and negligible pressure drop, the partial pressures in the gas phase at any position and instant of time are obtained by solving the following set of partial differential equations for each of the species *i* in the gas mixture.

$$\frac{1}{RT}\varepsilon\frac{\partial P_i}{\partial t} = -\frac{1}{RT}\frac{\partial (uP_i)}{\partial z} - (1-\varepsilon)\rho\frac{\partial q_i}{\partial t} \quad ; \quad i = 1, 2 \qquad (2)$$

In equation (2), *t* is the time, z is the distance along the adsorber, ρ is the framework density, ε is the bed voidage, and u is the superficial gas velocity. The molar loadings of the species *i*, q_i, at any position *z*, and time *t* is determined from the IAST calculations. Details of the numerical procedures used are available in earlier works.[5,6,7] In the breakthrough calculation the following parameter values were used: bed length, L = 0.3 m; voidage of bed, ε = 0.4; superficial gas velocity and u = 0.04 ms^{-1} (at inlet). The framework density of **UTSA-48a** is 748.9 kg m^{-3}.

[5] Krishna, R.; Long, J. R. *J. Phys. Chem. C.* **2011**, *115*, 12941.

[6] Walton, K. S.; LeVan, M. D. *Ind. Eng. Chem. Res* **2003**, *42*, 6938.

[7] Krishna, R.; Baur, R. *Sep. Purif. Technol.* **2003**, *33*, 213.

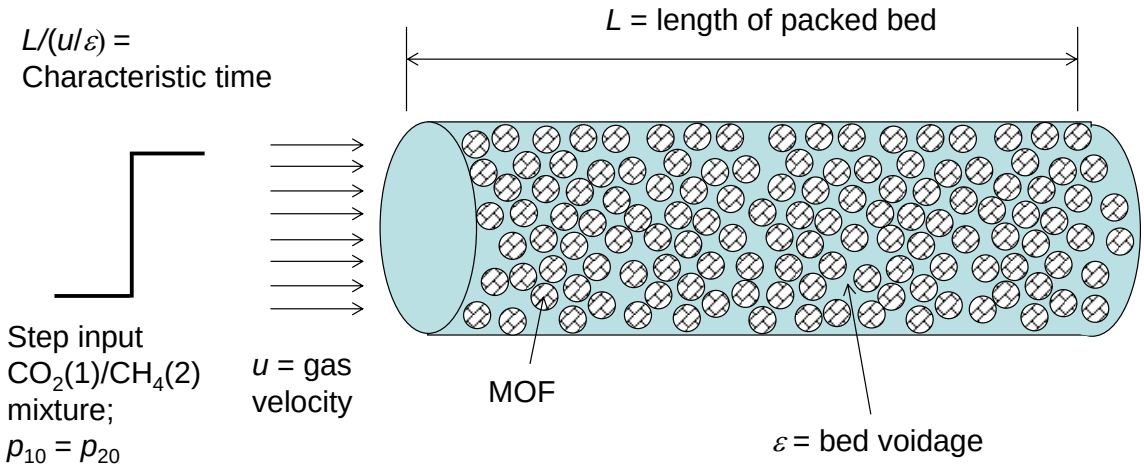

Figure S4. Schematic of a packed bed adsorber.

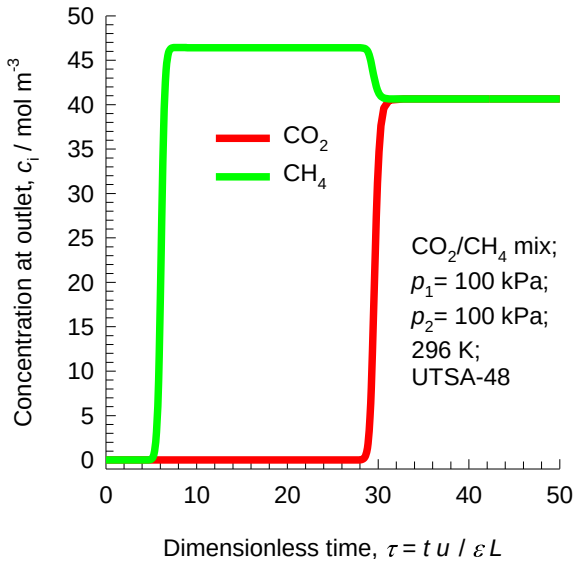

Figure S5. UTSA-48 maintained at isothermal conditions at 296 K. In this calculation, the partial pressures of CO_2 and CH_4 at the inlet is taken to be $P_1 = P_2 = 100$ kPa.

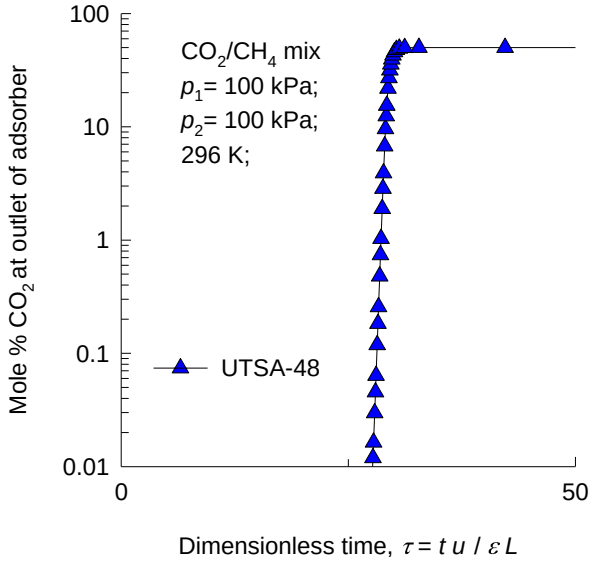

Figure S6. Plot of the number of molecules of CO_2 captured per litre of adsorbent material during the time interval O-τ_{break} against the breakthrough time τ_{break} for packed bed adsorber with step – input of a 50/50 CO_2/CH_4 mixture at 296 K and total pressures of 200 kPa. The breakthrough times, τ_{break}, correspond to those when the outlet gas contains 0.05 mole% CO_2.

Table S2. Dual-site Langmuir parameter for adsorption of CO_2, and CH_4 in **UTSA-48a**

	Site A				Site B			
	$q_{A,sat}$ mol kg^{-1}	b_{A0} Pa$^{-\nu_i}$	E_A kJ mol^{-1}	ν_A dimensionless	$q_{B,sat}$ mol kg^{-1}	b_{B0} Pa$^{-\nu_i}$	E_B kJ mol^{-1}	ν_B dimensionless
CO_2	0.15	3.88×10^{-8}	20	1	3.2	1.45×10^{-9}	20	1
CH_4	1.8	8.44×10^{-10}	18	1				